Synthesis and Characterization of New Co(II), Rh(III) and Pt(II) Guanidine and Thiourea Complexes†

Weihao Da,[a] T. Harri Jones,[a] J.-B. Lin,[b] Barry A. Blight*[a]

[a] Department of Chemistry, University of New Brunswick, Fredericton, NB, E3B 5A3, Canada

[b] Centre for Chemical Analysis, Research and Training Memorial University, St. John's, NL, Canada, A1B 3X7

* Corresponding author: b.blight@unb.ca

† Dedicated to the life and work of the late Prof. Suning Wang; a leader, a colleague, a mentor.

ABSTRACT:

Guanidine and thiourea based complexes have been the subject of extensive study due to their wide range of potential applications including but not limited to anti-cancer drugs, ion transporters and sensors. Building upon previous work done in this group, we aimed to demonstrate a new series of organo-metallic complexes based around functionally diverse guanidine and thiourea ligands. Herein the synthesis and characterisation of these new platinum, rhodium and cobalt complexes is presented. While most of these complexes conformed to properties and behaviours in line with predictions based upon previous work, one complex based around a Pt (II) and a guanidine derivative exhibited unusual supramolecular properties; demonstrating a larger self-assembly of 6 Pt (II) cations.

KEYWORDS: H-Bonding, Coordination Compounds, Second-Sphere Interactions

Introduction

Thiourea and guanidine derivatives have the general formulae of $(NR_2)_2CS$ and $(R_2N)_2C{=}N{-}R_5$ respectively.[1-5] They been extensively studied in complex chemistry[6-7] and have been proven to have applications as chemical sensors,[8-10] catalysts,[8,11] ion transporters[13-14] and several have been studied as anti-cancer drugs.[11,15-17] Adjacent to this area, thioureas and guanidine as ligands bound to metal complexes have been reported and their metal-ligand coordination behaviour studied; Vijayan et al[6] introduced Ruthenium (II) complexes containing thiourea derivatives, which showed interesting biological properties, particular in anti-cancer research.[6] Bailey and Pace[7] synthesised Pt and Ir complexes containing guanidine derivatives, illustrating the diversity of metals that can be coordinated (both transition and main group) and variations in the nature of the coordination in which these guanidine derivatives ligands bind.[6-7,18-19] Structurally, both thiourea and guanidine ligands have two parallel-disposed NH groups, and as such, some metal-containing Thiourea or Guanidine complexes have been used to study hydrogen-bonding with complementary H-bonding partners.[20]

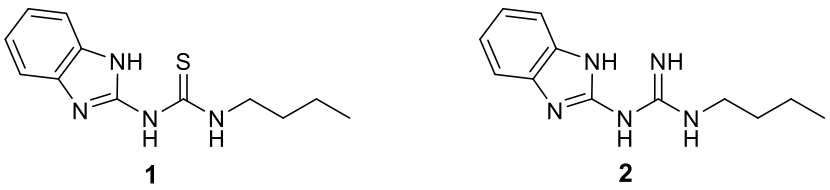

Figure 1. Structure of benzimidazole Thiourea 1 and Guanidine 2 ligands previously used in the Blight group.[21]

Previous work in our group has centred around the study of Ir (III) guanidine and thiourea based complexes as photo-active molecules capable of H-bonding.[21-22] How the H-bonding impacts on the photoactivity of the complexes was also studied along with the strength of the binding. Herein, we present several complexes, centred around Rh (III), Co (II) and Pt (II) metals. These complexes were characterised using mass spectrometry, CHN combustion

analysis and NMR spectroscopy. The structures of each complex were also identified using single crystal X-ray diffraction techniques. The coordination of these complexes is mostly consistent between the guanidine/ thiourea groups being 2-coordinate. The exception is for Pt (II) complex 5, which can form a larger supramolecular oligomer between multiple repeating units of the complex.

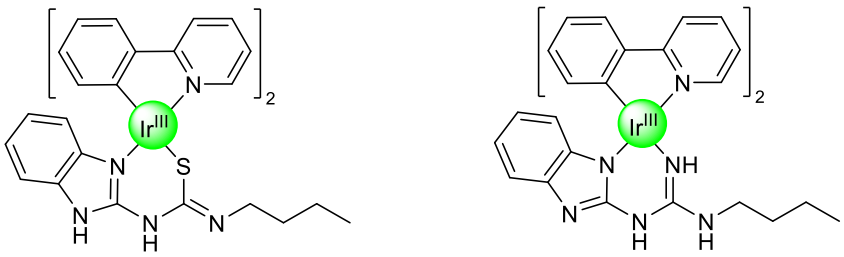

Figure 2. Structures of previously reported Ir (III) Thiourea and Guanidine complexes.[21-22]

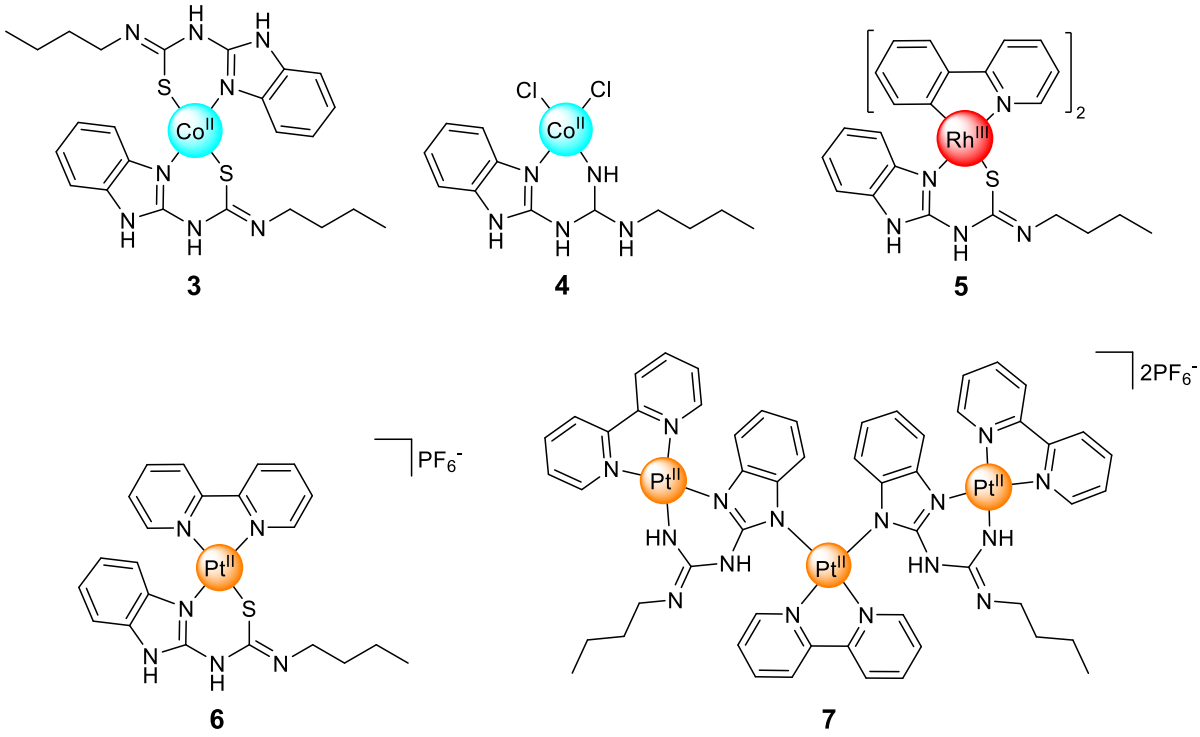

Figure 3. Structures Co (II) complex 3 and 4, Rh (III) complex 5 and Pt (II) complexes 6 and 7 to be discussed.

Experimental

Materials. All solvents and starting materials were purchased from Fisher Scientific, Sigma-Aldrich, Arcos Organics and Alfa Aesar. These materials were used as received from the supplier without any further purification unless otherwise stated. All compound reactions were carried out under nitrogen atmosphere unless stated otherwise.

NMR. ^{1}H NMR (400 MHz) and ^{13}C NMR (100 MHz) spectra were recorded on an OXFORD 400 NMR spectrometer with deuterated solvents DMSO-d_6 and chloroform-d used as noted. All chemical shifts are reported in δ (ppm) to using residual solvent as reference, while peak multiplicities are referred to as singlet (s), doublet (d), triplet (t), quartet (q), broad singlet (bs), and multiplet (m).

Mass Spectrometry. High-resolution mass spectral data measurements were performed by the Mass Spectrometry Laboratory, Dalhousie University, Halifax, Nova Scotia, Canada. High-resolution mass spectra were recorded on a Bruker Daltonics MicrOTOF instrument. The ionization method used for low-res and high-res analysis was positive or negative electrospray ionization (ESI). The sample was introduced by a syringe pump at a flow rate of 2 μL/min. The spray voltage applied to the ESI needle was 4.5 kV. The dry gas flow rate was 4 L/min. Nebulizer gas was 1 bar and source temperature 180°C.

Elemental Analysis. Elemental analysis was performed by the Centre for Environmental Analysis and Remediation, Saint Mary's University, Halifax, Nova Scotia, Canada. Carbon, hydrogen, and nitrogen analyses were carried out on a Perkin Elmer 2400 Series II CHN Analyzer. Results were obtained as a percentage by weight and were measured as a function of thermal conductivity.

Single Crystal X-ray Diffraction Analysis

Single-crystal X-ray diffraction data was collected at the Centre for Chemical Analysis, Research and Training (C-CART) Memorial University, St. John's, NL, Canada, A1B 3X7. Collected at 100(2) K on a Rigaku XtaLAB Synergy-S, Dualflex, HyPix-6000HE diffractometer using Cu K radiation (λ = 1.5406 Å). The crystal was mounted on a nylon CryoLoop with Paraton-N. The data collection and reduction were processed within CrysAlisPro (Rigaku OD, 2019). A Gaussian absorption correction was applied to the collected reflections. Using Olex2,[1] the structure was solved with the ShelXT[2] structure solution program using Intrinsic Phasing and refined with the ShelXL[3] refinement package using Least Squares minimization. All non-hydrogen atoms were refined anisotropically. The azole and amine hydrogen atoms were located in difference Fourier maps and refined by using the DFIX and HTAB commands. All other organic hydrogen atoms were generated geometrically. Solvent mask was applied to the disordered solvent. Each data set has been uploaded to the Cambridge Crystallographic Data Centre as entries: XXXXX (**4**), XXXXX (**5**), XXXXX (**6**), XXXXX (**7**).

Synthetic Procedures

Synthesis of both Thiourea and Guanidine ligands (**1** and **2**) were prepared according to previous published work.[21-22]

Cobalt complex 3. Cobalt (II) chloride hexahydrate $CoCl_2 \cdot 6H_2O$ (30 mg, 0.126 mmol) and Ligand **1** (28 mg, 0.112 mmol,0.9 equiv.) were added to 10 mL of methanol. The reaction mixture was stirred overnight at 80°C for 24 h under a N_2 atmosphere. After cooling down to room temperature, the solvent was removed under reduced pressure. Water was added (50 mL), and the mixture was sonicated, and then filtered via Buchner funnel. The filtrate was

thoroughly washed with water. The final product was further purified via precipitation (chloroform/hexane), dried under vacuum, and obtained as dark green powder with a 56% yield.

^{1}H-NMR (400 MHz, DMSO-d^{6}) δ 7.14 (s, 1H), 6.91 (s, 1H), 6.69 (s, 1H), 3.37 (s, 2H), 1.43 (s, 2H), 1.31 (s, 2H), 0.87 (t, 3H). Electrospray mass-spectroscopic analysis: m/z=553.1. Elemental analysis: expected: C is 52.07%, H is 5.46%, N is 20.24%; actual: C is 52.11%, H is 5.61%, N is 20.16%.

Cobalt complex 4. Cobalt (II) chloride hexahydrate $CoCl_2 \cdot 6H_2O$ (30 mg, 0.126 mmol) and Ligand **2** (26 mg, 0.112 mmol, 0.9 equiv.) were added to 10 ml of methanol. The reaction mixture was stirred overnight at 80°C for 24 h under the N_2 atmosphere. After cooling to room temperature, the solvent was removed under reduced pressure. Water was added, and the mixture was sonicated, and then filtered via Buchner funnel. The filtrate was thoroughly washed with water and DCM. Final product was dried under vacuum and obtained as bright blue powder in 49% yield.

^{1}H-NMR (400 MHz, DMSO-d^{6}) δ 11.12 (s, 1H), δ 7.48 (s, 1H), 7.03 (s, 1H), 3.63 (s,2H), 1.57 (m, 2H), 1.43 (m, 2H), 0.96 (t, 3H) (Figure 2.9). Elemental analysis: expected: C is 39.91%, H is 4.74%, N is 19.39%; actual: C is 40.01%, H is 4.60%, N is 19.31%

Rh (III) complex 5. A Rhodium Ppy dimer [23] (50 mg, 0.056 mmol), Ligand **1** (35 mg, 0.141 mmol,2.5 equiv.), and potassium carbonate (75 mg, 0.543 mmol, 10 equiv.) were added to 15 mL of dry toluene. The reaction was refluxed for 24 h under the N_2 atmosphere. After cooling to room temperature, the solvent was removed under reduced pressure. The precipitate was then dissolved in DCM (20 mL). The mixture was extracted with water (3 x 20 mL) to remove the excess base. The organic layers were combined, dried over magnesium sulphate, filtered, and the solvent was removed under reduced pressure. Further purification included

column chromatography (silica gel, CH_2Cl_2/MeOH). Final product was obtained as light-yellow green powder in 49% yield.

^{1}H-NMR (400 MHz, DMSO-d^6) δ 9.04 (d, 1H), 8.54 (s, 1H), 8.08 (d, 1H), 7.91 (d, 1H), 7.85 (s, 1H), 7.81 (d, 1H), 7.61 (m, 1H), 7.56 (d, 1H), 7.23 (d, 1H), 7.14 (d, 1H), 7.05 (d, 1H), 7.01 (d, 1H), 6.96 (d, 2H), 6.91 (d, 1H), 6.86 (d, 1H), 6.78 (d, 1H), 6.65 (m, 1H), 6.42 (d, 1H), 6.31 (d, 1H), 6.18 (d, 1H), 3.46 (dt, 2H), 1.56 (q, 2H), 1.32 (dq, 2H), 0.85 (t, 3H). ^{13}C-NMR (101 MHz, CDCl3) δ 171.42, 169.87, 169.56, 165.68, 164.58, 164.56, 156.08, 151.00, 149.94, 144.43, 143.58, 142.53, 137.33, 136.79, 132.58, 131.62, 128.39, 128.22, 124.03, 123.50, 122.07, 121.92, 121.79, 121.04, 119.15, 115.66, 108.58, 41.66, 31.26, 19.68, 13.82 Electrospray mass-spectroscopic analysis: calc: m/z = xyz; actual: m/z=659.15. Elemental analysis: expected: C is 62.00%, H is 4.74%, N is 12.76%; actual: C is 61.26%, H is 4.74%, N is 12.43%.

Pt (II) complex 6. (2,2′-Bipyridine) dichloroplatinum (II) (30 mg, 0.071 mmol) [24] and Ligand **1** (19.5 mg, 0.079 mmol, 1.1 equiv.) were added to 10 ml dry dimethylformamide. The reaction mixture was stirred overnight at 80°C for 24 h under the N_2 atmosphere. After cooling down to room temperature, the solvent was removed under reduced pressure. Ion exchange was performed via KPF_6. Extraction was done with dichloromethane and water. Organic phases were combined, dried over magnesium sulphate, filtered, and solvent was removed under reduced pressure. Product was further purified via trituration in hexane, filtration and dried under vacuum. Final product was obtained as chrome yellow powder in 68% yield.

^{1}H-NMR (400 MHz, DMSO-d^6) δ 12.69 (s, 1H), 9.08 (dd, 1H), 8.79 (t, 1H), 8.73 (m, 4H), 8.51 (d, 1H), 8.44 (m, 3H), 7.91 (ddt, 1H), 7.63 (m, 1H), 7.36 (d, 1H), 7.30 (d, 1H), 7.20 (t, 1H), 7.10 (td, 1H), 3.36 (m, 2H), 1.58 (m, 2H), 1.35 (q, 2H), 0.92 (t, 3H). ^{13}C-NMR (101

MHz, DMSO-d^6) δ 165.44, 157.87, 155.79, 155.05, 150.18, 148.77, 141.90, 141.70, 137.64, 133.31, 128.35, 128.01, 125.18, 124.81, 123.26, 122.25, 116.03, 111.64, 43.14, 30.91, 20.17, 14.15.

Electrospray mass-spectroscopic analysis: calc: m/z = xyz; actual: m/z = 589.1. Elemental analysis: expected: C is 35.54%, H is 3.12%, N is 11.30%; actual: C is 35.59%, H is 3.18%, N is 11.04%.

Pt (II) complex 7. Ligand **2** (13 mg, 0.052 mmol), (2,2′-Bipyridine) dichloroplatinum(II) [24] (30 mg, 0.078 mmol,1.5 equiv.), cesium carbonate (34 mg, 0.104 mmol, 2 equiv.) were added to 10 ml dry dimethylformamide. The reaction mixture was stirred overnight at 80°C for 24h under the N_2 atmosphere. After cooling down to room temperature, the solvent was removed under reduced pressure. Ion exchange was performed via KPF_6. Extraction was done with dichloromethane and water. Organic phases were combined, dried over magnesium sulphate, filtered, and solvent was removed under reduced pressure. Product was further purified via trituration in hexane, filtration and dried under vacuum. Final product was obtained as crimson powder in 51 % yield.

Electrospray mass-spectroscopic analysis calc: m/z = xyz; actual: m/z = 755.7. Elemental analysis: expected: C is 35.99%, H is 3.02%, N is 12.43%; actual: C is 36.02%, H is 3.28%, N is 12.54%.

Results and discussion

The synthesis of the Co (II) complexes **3** and **4** were completed by refluxing reagents in methanol under nitrogen overnight. The coordination environments of these two cobalt centred complexes behave very differently. Cobalt (II) being paramagnetic in both low spin and high spin states means that the NMR data acquired is tentative. Therefore, further analysis was based on CHN mass spectrometry and in the case of complex **4** single crystal X-

ray diffraction. The cobalt centre in complex **3** is coordinated by two thiourea ligands while complex **4** is only coordinated by a single guanidine ligand. The binding of complex **3** is perceived to have one anionic ligand and one neutral ligand binding through each of the sulphide groups of the thiourea moieties, and one dative coordination through the nitrogen. As noted above, however, the paramagnetic nature of this material precludes structural confirmation by ^{1}H NMR and the structure derived the mass spectrometry and combustion analysis data alone.

In the case of complex **4**, both coordinate bonds from the guanidine ligand are dative, while the Co (II) binds two chlorides to stabilise the charge. Unlike with complex **3**, for complex **4** we were able to obtain a single crystal X-ray to make observations on the nature of the ligand coordination (shown in figure 4). The most important intermolecular bonds of complex **4** are the H-bonds between the chlorides and the hydrogens (H5…Cl2 = 2.815(5) Å) and (H1…Cl1 = 2.530 (3) Å). This distance is shorter than the sum of the Van der Waals radii of the atoms indicating H-bonding. This bond, along with the distorted tetrahedral geometry of the Cobalt (II) centre allows for asymmetrical stacking of molecules of the complex.

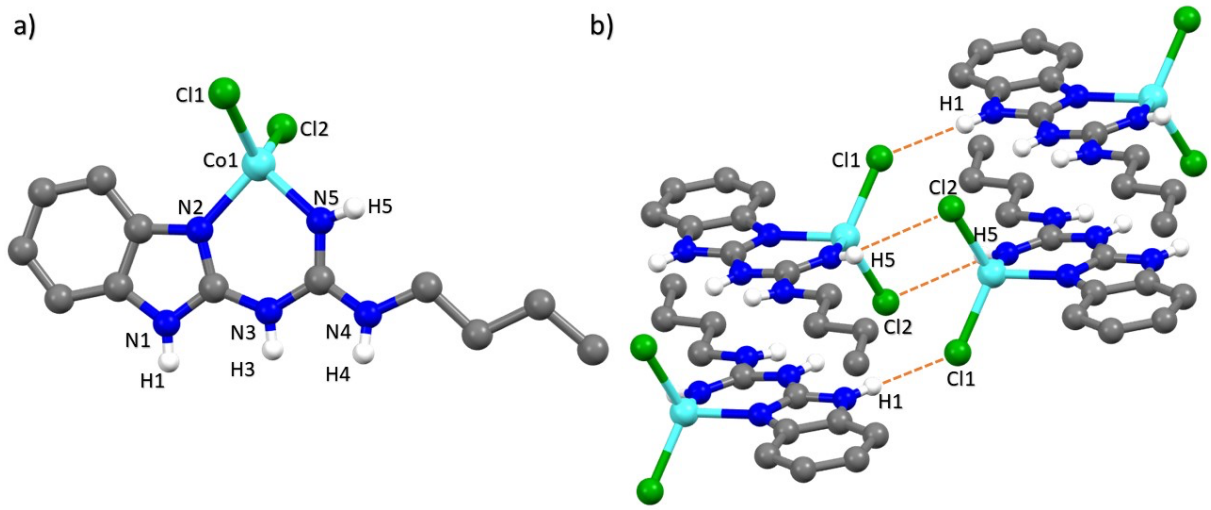

Figure 4. a) Resolved molecular structure of cobalt (II) complex **4.** Crystallized in P-1 space group, triclinic. CHs removed for clarity. (Grey: carbon; blue: nitrogen; white: hydrogen; cyan: cobalt (II);

green: chlorine) **b)** Stacking of several molecules of complex 4 with labels of H-bonding interactions (H5…Cl2 = 2.815(5) Å) and (H1…Cl1 = 2.530 (3) Å)

Complex **5** was synthesised through the reaction of a Rh (III) dimer, [23] akin to the isostructural Ir(III) chloro-bridged dimer, [21] with ligand **2**. The complex was identified using mass spectrometry and NMR spectroscopy, but further investigated using single crystal X-ray diffraction. Complex **5** crystallized in $P2_1/n$ space group, monoclinic. The Rh (III) is bonded to two phenyl pyridine ligands through bidentate C^N ligation and to the Thiourea ligand forming a 6-membered chelate.

The coordination geometry and binding of the ligands to the Rh (III) centre behaves almost identically to previous Iridium (III) based cyclo-metallic compounds studied in this group. [21] Two molecules of complex **5** can self-recognise through H-bonding within the lattice (shown below in Figure 6), the intermolecular bond distances of the two molecules of complex **5** are (N1…N9 = 2.948(9) Å) and (N3…N7 = 2.919(10) Å). These distances are less than the sum of the Van der Waals radii, indicating that H-bonding is occurring between the two molecules of complex **5**. It is worth noting that these self-recognising intermolecular bond distances are smaller than the Iridium structures in previous work, which had comparable intermolecular bond distances of 2.76 Å and 2.91 Å. [21]. Due to the similarity of results, we were prompted us to undertake binding studies to determine the strength of these H-bonding interactions.

Comparing the photophysical data on the compounds reveals intense bands around 250 - 300 nm in both compounds which are assumed to be weak π−π* transitions. The next emission bands were around 320 nm and 350 nm. With the increase in concentration of **8** it was found that the emissions at 320 nm decreased while the emissions at 350 nm increased showing clear changes to the photo luminescent properties of Rh (III) complex **3**. In order to investigate the strength of the H-bonding of the ancillary ligand, pyrimido-[4,5-c]isoquinolin-3-amine (herein referred to as **8** shown in scheme below) was introduced through titrations to

observe the effects that a triplet H-bonded species would have on the photophysical properties of complex **5**. [21-22,25] The experimental binding constant K_a was determined to be 1.1 x 10^3 M^{-1} ± 0.1 %. In previous work on Iridium (III) compounds with identical ligands in the presence of compound **8**, it was found that the binding constant K_a was more than three times stronger. This indicates that this Rhodium complexes H-bonding was much weaker than previous Iridium species studied. [21-22]

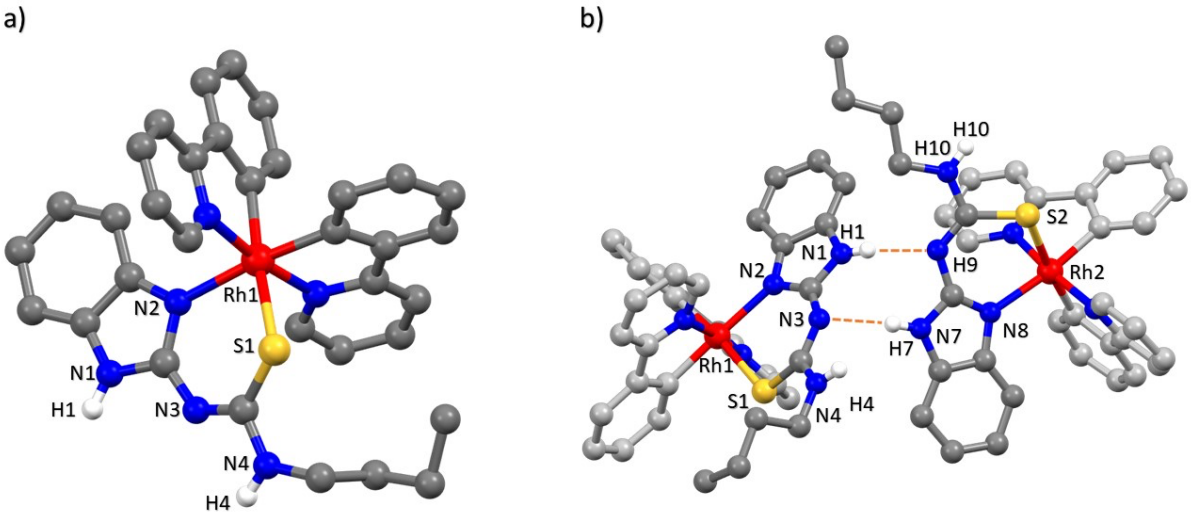

Figure 5. a) Resolved molecular structure of rhodium (III) complex **5**. CHs removed for clarity. Crystallized in P21/n space group, monoclinic. (Grey: carbon and light grey; blue: nitrogen; white: hydrogen; red: rhodium (III); yellow: sulfur) **b)** Dimeric form of complex 5 with labels of H-bonding interactions (N1…N9 = 2.948(9) Å) and (N3…N7 = 2.919(10) Å)

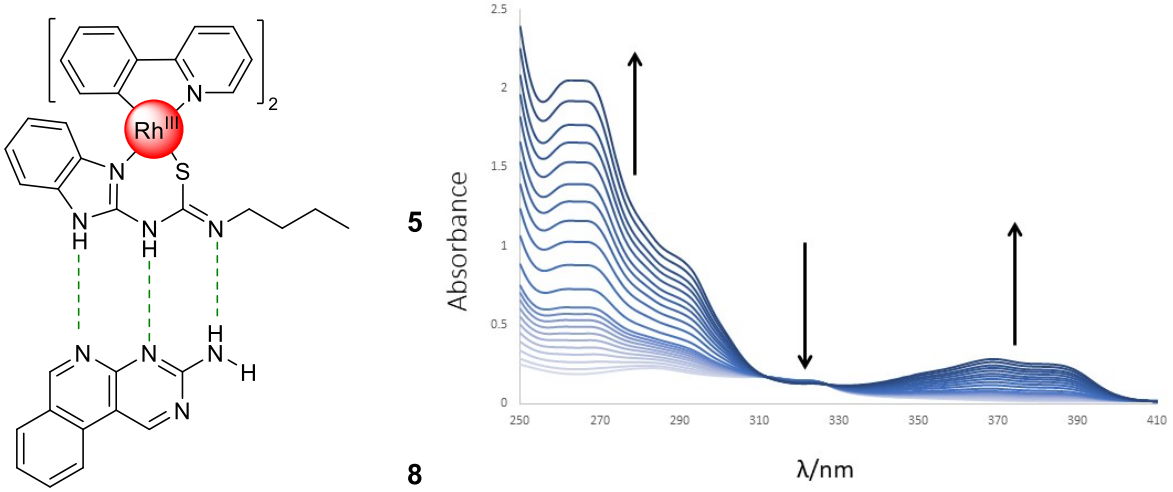

Figure 6. Rh (III) complex 5 binding to 8 (left) and results from experimental UV-vis binding study in 99 % chloroform & 1 % DMSO of complex 5 with 8 with arrows indicating the change in absorbance as the concentration of 8 was increased (right).

The final two complexes discussed here are both synthesised through the complexation of ligands **1** or **2** with a Pt (II) chloro-bridged dimer starting material.[24] Complex **6** and **7** were both identified using ^{1}H and ^{13}C NMR and mass spectrometry (see SI). Single crystals were also obtained for both complexes **6** and **7** and X-ray diffraction was used to analyse the specific binding of the molecules.

Single crystals of compound **6** were obtained through slow vapour diffusion of hexanes into a chloroform solution of Pt (II) affording complex **6** crystallizing in the triclinic P-1 space group. Crystals appeared as yellow starburst clusters, with a structural solution containing a central Pt (II) bound to a bipyridine ligand and butyl Thiourea benzimidazole ligand in a distorted square planar geometry. Complex **6** exhibits π-π stacking between two adjacent bipyridines and the ring of the benzimidazoles. The distance between the planes formed by the bipyridines is 3.245 Å and the distance between the two five members aromatic rings of the benzimidazole, it is 3.334. These structures also have the capability of self-recognising through their H-bonding sites on the Thiourea ligand. As shown in Figure 7, two molecules of complex **6** can H-bond with the same PF_6^- ion, with bond lengths between (H2…F11 = 2.240(3) Å), and (H8…F12 = 2.597(2) Å). These H-bonding interactions contribute to the larger self-assembled structure forming.

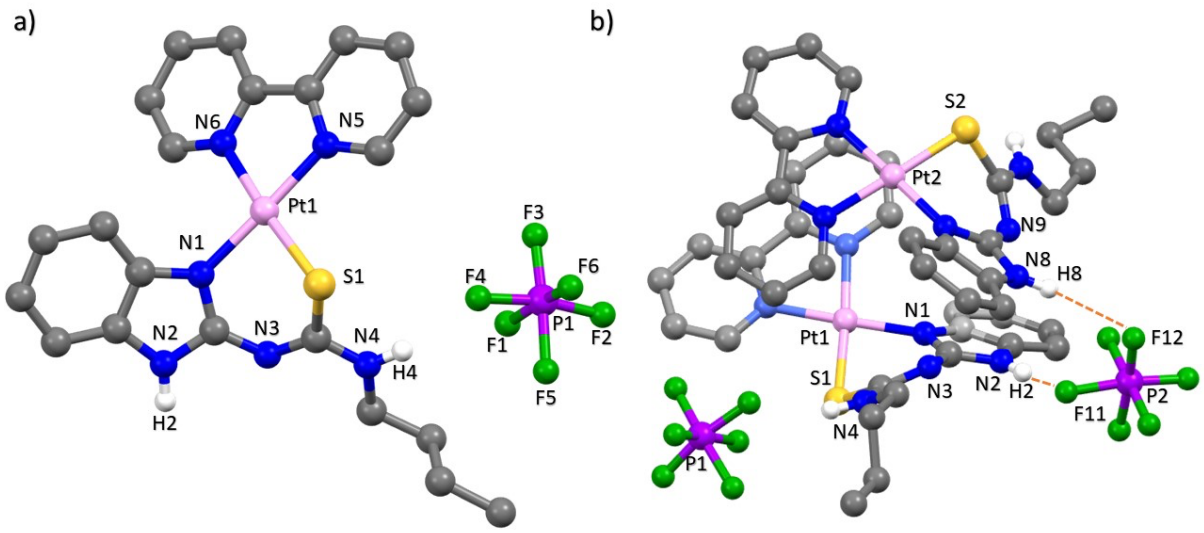

Figure 7. a) Resolved molecular structure of platinum (II) complex **6.** Crystallized in P-1 space group, triclinic. CHs removed for clarity. (Grey: carbon; blue: nitrogen; white: hydrogen; pink: platinum (II); yellow: sulfur; purple: phosphorus; green: fluorine) **b)** Larger assembly of complex 6 shown H-bonding with the PF_6^- ion (H2…F11 = 2.240(3) Å), and (H8…F12 = 2.597(2) Å)

Complex **7** was synthesised using the noted Pt (II) chloro dimer [24] and ligand **1**. The analysis of the product gave an unexpected result. It was assumed that complex **7** would behave much like complex **6** in forming single complexes with bipyridine and thiourea. However, the ^{1}H NMR data was inconclusive and indicated polymeric behaviour. It was found upon X-ray diffraction of a single crystals that the product had formed a larger self-assembly where three Pt (II) cations are coordinated to two thiourea ligands and three bipyridine ligands (Figure 8). Additionally, the mass spectrometry data indicates two major products; a trimetallic species with m/z value of 1512.37 and a monometallic species with a m/z value of 581.2, which is the mass value for the expected structure.

Upon further observation it's clear that the bipyridines of the Pt (II) trimer are stacking to form a larger supramolecular self-assembly through π-π stacking leading to a remarkable alpha-helix shape. The contact distances of π-π stacking between two bipyridine planes are (C45…C64 = 3.128(7) Å), (C52…C56 = 3.649(7) Å), (C10…C99 = 3.297(3) Å), (C3…C106

= 3.345(8) Å) and the contact distances of metal atom (Pt) -π are 3.419 Å (C8…Pt6 = 3.311(4) Å), (Pt4…C47 = 3.311(3) Å). One interesting feature for potential further study is the cavity that forms between the interlocked trimers, this cavity may be applicable for small molecule coordination or potential transformations.

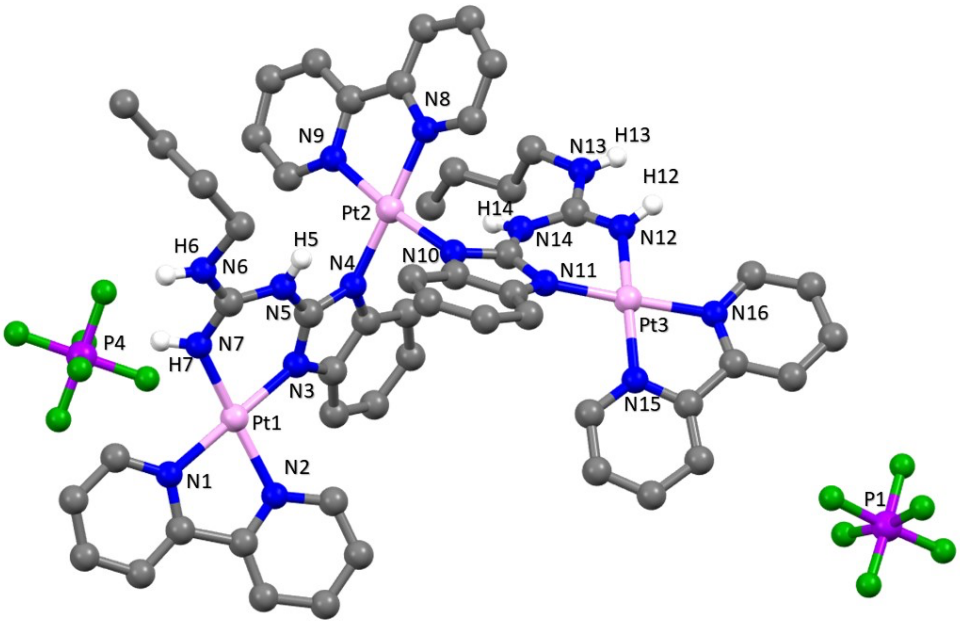

Figure 8. Resolved molecular structure of platinum (II) complex **7.** CHs removed for clarity. Crystallized in I2/a space group space group, monoclinic. (Grey: carbon; blue: nitrogen; white: hydrogen; pink: platinum (II); purple: phosphorus; green: fluorine)

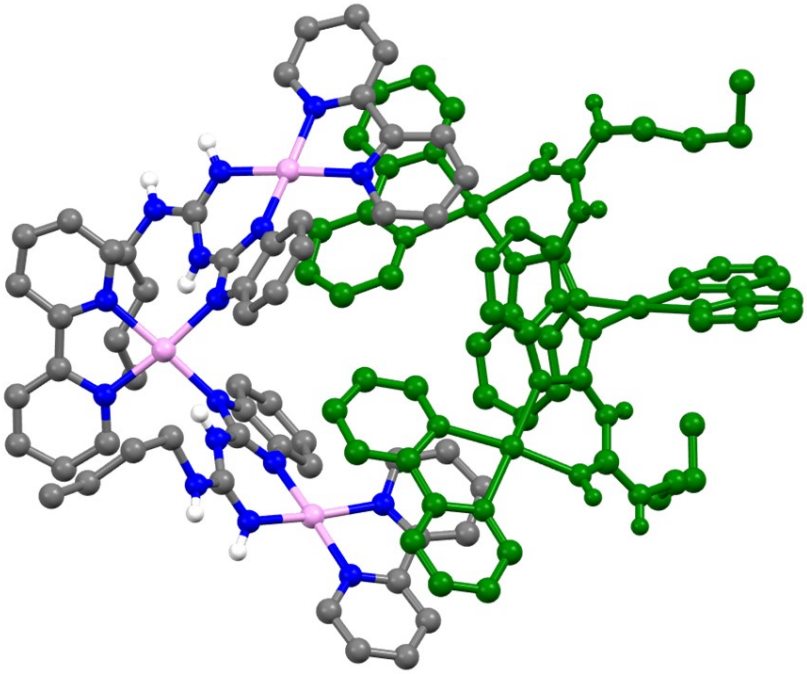

Figure 9. Two different perspectives of complex 7. The two molecules are coloured monochromatically to show the specific formation of the helical like supramolecular metallo-foldamer.

In DMSO, this platinum (II) trimetallic complex **7** appears to be in dynamic equilibrium between the large supramolecular assembly and the simpler trimetallic form. This polar solvent will favour π-π stacking interactions resulting in varied proton environments resulting in broader peaks shown in the ^{1}H NMR.

This self-assembled super-complex behaves in a similar fashion to that of a Pd (II) metallo-foldamer investigated by Preston *et al.*[26] Like the foldamer synthesised by Preston *et al.* this strucutre exhibits a helical geometry around the square planar metal cations. The difference being that the structures full supramolecular assembly is only realised once two monomers of the trimetallic complex **7** bind together to form the 6 Platinum (II) super structure, where as Preston *et al'*s structures do not feature this self recognition between two monomers. This feature leads to the formation of a modest-sized cavity, which has some similarities to that of a double bowl metallocavitand,[27] this cavity may be a good subject for further investigation into small molecule binding or catalysis.

Conclusions

This work identified and discussed five new unique thiourea- and guanidine-based metal complexes with novel H-bonding properties. Complex **3**, **4**, **6** and **7** were all 4-coordinate in nature with some ability for self-recognition due to their H-bonding abilities. Complex **5** was octahedral and exhibited similar behaviour to the Ir (III) complexes previously synthesised by the Blight group.[21-22] All complexes exhibit bidentate coordination through the thiourea/ guanidine ligands *via* the sulphide/ nitrogen atoms. Complex **7** showed, through intermolecular H-bonding and pi-stacking, a possible supramolecular oligomer with a small cavity, that requires further investigations into what could possibly bind in the space.

Author Contributions

The manuscript was written through contributions of all authors. In addition, BAB devised the experiments, while WD carried out all experiments. THJ helped assemble the final manuscript.

Funding Sources

We gratefully acknowledge the University of New Brunswick, and its Department of Chemistry for financial and technical support. This work was fully supported by Natural Science and Engineering Council of Canada (NSERC; DG RGPIN-2018-04021) and New Brunswick Foundation for Innovation (NBIF; RAI-2019-023).

References

[1]- Güthner, T.; Mertschenk, B.; Schulz, B.; “Guanidine and Derivatives”inUllmann's Encyclopedia of Industrial Chemistry, Wiley-VCH, Weinheim,Germany,**2012**, 17, 175–189

[2]- Kiesewetter, M.K.; Scholten, M.D.; Kirn, N.; Weber, R.L.; Hedrick, J.L.; Waymouth, R.M.; *J. Org. Chem*. **2009**, 74, 24, 9490-9496

[3]- Cui, X.Y.; Tan, C.H.; Leow, D.; *Org. Biomol. Chem*. **2019,** 17, 4689-4699

[4]- Nolting, D.; Ottosson, O.; Faubel, M.; Hertel, I.V.; Winter, B.; *J. Am. Chem. Soc.* **2008**, 130, 8150–8151.

[5]- Boyle, E. M.; Comby, S.; Molloy, J. K.; Gunnlaugsson, T. *J. Org. Chem.* **2013**, 78, 8312-8319.

[6]- Premkumar, M.; Vijayan, P.; & Venkatachalam, G.; *J. Organomet. Chem.* **2019**, 902, 120964.

[7]- Bailey, P. J.; Pace, S.; *Coord. Chem. Rev*. **2001**, 214, 91-141.

[8]- Kim, H.; Lim, H.K.; Cho, S.; Kim, H.J.; *J. Photochem. Photobiol. A Chem.* **2019**, 383, 112023.

[9]- Siva, V.; Shameem, A.; Murugan, S.; Athimoolam, G.; Vinitha, S.; Bahadur, A.; *Chinese J. Phys.* **2020**, 68, 764–777.

[10]- Durmaz, M.; Acikbas, Y.;Bozkurt, S.; Capan, R.; Erdogan, M.; Ozkaya, C.; *ChemistrySelect.* **2021**, 6, 4670 –4676.

[11]- Zhang, S.; He, L.N.; *Aust. J. Chem.* **2014**, 67, 980-988.

[12]- Yan, T.; Zheng, X.; Liu, S.; Zou, Y.; Liu, X.; J. *Sci. China Chem.* **2022**, 65, 1265–1278.

[13]- Sherazi, T. A.; Zahoor, S.; Raza, R.; Shaikh, A.J.; Naqvi, S.A.; Khan, G.A.; Li, S.; *Int.*

J. Hydrogen Energy. **2015**, 40, 786–796 (2015).

[14]- Zhao, Z.; Tang, B.; Yan, X.; Wu, X.; Li, Z.; Gale, P.A.; Jiang, Y.B.; *Front. Chem. Sci. Eng.* **2022**, 16, 81–91.

[15]- Lv, P.C.; Li, H.Q.; Sun, J.; Zhou, Y.; Zhu, H.L.; *Bioorganic Med. Chem.* **2010**, 18, 4606–4614.

[16]- El-Razek, S.E.; El-Gamasy, S.M.; Hassan, M.; Abdel-Aziz, M.S.; Nasr, S.M.; *J. Mol. Struct.* **2020**, 1203, 127381.

[17]- Saczewski, F.; Balewski, Ł.; *Expert Opin. Ther. Pat.* **2013**, 23, 965–995.

[18]- Fairlie, D.P.; Jackson, W.G.; Skelton, B.W.; Wen, H.; White, A.H.; Wickramasinghe, W.A.; Woon, T.C.; Taube, H.; *Inorg. Chem.* , **1997**, 36, 1020–1028.

[19]- Reinmuth, M.; Walter, P.; Enders, M.; Kaifer, E.; Himmel, H. J.; *Eur. J. Inorg. Chem.* **2011**, 83–90.

[20]- Zhang, C.; Zeng, H.; Huang, Q.; Wang, Y.; Chai, Y.; Huang, Y.; Zhao, S.; Lu, Z.; *Material. J. Mater. Chem. C* **2018**, 6, 4095−4105.

[21]- Balónová, B.; Martir, D.R.; Clark, E.R.; Shepherd, H.J.; Zysman-Colman, E.; Blight, B.A.; *Inorg. Chem.* **2018**, 57, 8581–8587.

[22]- Balónová, B.; Blight, B. A.; *Front. Chem.* **2021**, 9, 1–6.

[23]- Sprouse, S.; King, K.A.; Spellane, P.J.; and Watts, R.J.; *J. Am. Chem. Soc.* **1984**, 6647–6653

[24]- Newkome, G. R.; Puckett, W. E.; Gupta, V. K.; Kiefer, G. E.; *Chem. Rev.* **1986,** 86, 451–489.

[25]- Supramolecular BindFit. www.supramolecular.org.

[26]- Preston, D.; *Angew. Chemie - Int. Ed.* **2021**, 60, 20027–20035 (2021).

[27]- Yu, S.-Y.; Huang, H.; Liu, H.-B.; Chen, Z.-N.; Zhang, R.; Fujita, M.; *Angew. Chemie - Int.*, **2003**, 42(6), 686–690.